

The Lopsidedness of Present-Day Galaxies: Connections to the Formation of Stars, the Chemical Evolution of Galaxies, and the Growth of Black Holes

Timothy A. Reichard¹, Timothy M. Heckman¹, Gregory Rudnick^{2,5}, Jarle Brinchmann³,
Guinevere Kauffmann⁴, Vivienne Wild⁴

ABSTRACT

A global lopsidedness in the distribution of the stars and gas is common in galaxies. It is believed to trace a non-equilibrium dynamical state caused by mergers, tidal interactions, asymmetric accretion of gas, or asymmetries related to the dark matter halo. We have used the Sloan Digital Sky Survey (SDSS) to undertake an investigation of lopsidedness in a sample of $\sim 25,000$ nearby galaxies ($z < 0.06$). We use the $m = 1$ azimuthal Fourier mode between the 50% and 90% light radii as our measure of lopsidedness. The SDSS spectra are used to measure the properties of the stars, gas, and black hole in the central-most few-kpc-scale region. We show that there is a strong link between lopsidedness in the outer parts of the galactic disk and the youth of the stellar population in the central region. This link is independent of the other structural properties of the galaxy. These results provide a robust statistical characterization of the connections between accretion/interactions/mergers and the resulting star formation. We also show that residuals in the galaxy mass-metallicity relation correlate with lopsidedness (at fixed mass, the more metal-poor galaxies are more lopsided). This suggests that the events causing lopsidedness and enhanced star formation deliver lower metallicity gas into the galaxy's central region. Finally, we find that there is a trend for the more powerful active galactic nuclei (the more rapidly growing black holes) to be hosted by more lopsided galaxies (at fixed galaxy mass, density, or concentration). However if we compare samples

¹Department of Physics and Astronomy, The Johns Hopkins University, 3400 North Charles Street, Baltimore, MD 21218-2686.

²National Optical Astronomy Observatory (NOAO), 950 N. Cherry Ave., Tucson, AZ 85719, USA

³Leiden Observatory, Leiden University, P.O. Box 9513, 2300 RA, Leiden, The Netherlands.

⁴Max-Planck-Institut für Astrophysik, D-85748 Garching, Germany.

⁵Goldberg Fellow

matched to have both the same structures *and central stellar populations*, we then find no difference in lopsidedness between active and non-active galaxies. Indeed the correlation between the youth of the stellar population and the rate of black hole growth is stronger than the correlation between lopsidedness and either of these other two properties. This leads to the following picture. The presence of cold gas in the central region of a galaxy (irrespective of its origin) is essential for both star-formation and black hole growth. The delivery of cold gas is aided by the processes that produce lopsidedness. Other processes on scales smaller than we can probe with our data are required to transport the gas to the black hole.

Subject headings: galaxies: structure, galaxies: interactions, galaxies: general

1. Introduction

In the standard Λ CDM universe, galaxies continue to grow significantly at the current epoch, accreting an average of roughly 5% of their mass per Giga-year (e.g., Kereš et al. 2005; Kauffmann et al. 2006). Minor mergers, tidal interactions with close companions, and asymmetric accretion of cold gas can all perturb the underlying structure of the dark matter halo, the stars, and the gas in galaxies for time-scales of-order a Giga-year (e.g., Zaritsky & Rix 1997; Levine & Sparke 1998; Jog 1999; Kornreich et al. 2002; Bournaud et al. 2005; Di Matteo et al. 2007; Mapelli et al. 2008; Cox et al. 2008).

A characteristic observational signature of these types of non-equilibrium situations is a global asymmetry (lopsidedness) in the distribution of the stars and/or gas. Indeed, galaxies commonly exhibit asymmetric structures. Asymmetry in the global H I 21cm emission-line profile is present in half or more of disk galaxies (Richter & Sancisi 1994; Matthews et al. 1998). Lopsided distributions of the H I gas are revealed by spatial maps of galaxies in the field (e.g., Swaters et al. 1999) and in groups (Angiras et al. 2006, 2007). The stellar mass distributions of disk galaxies are often lopsided as well. Zaritsky & Rix (1997) showed that $\sim 30\%$ of a sample of 60 field spiral galaxies had a significant $m = 1$ azimuthal Fourier component in the stellar mass. Rudnick & Rix (1998) showed that lopsidedness in the stellar mass distribution was common in early-type disk galaxies. Simulations of spiral galaxies have shown that the typical measured amplitudes of lopsidedness cannot be explained by internal dynamical mechanisms alone (e.g. Bournaud et al. 2005). The external processes described above are required.

It has long been recognized that tidal interactions and mergers can act as triggers

for star-formation (Toomre & Toomre 1972; Larson & Tinsley 1978). The resulting non-axisymmetric time-dependent gravitational potential can transport angular momentum out of the gas and also lead to shocks in which the gas is compressed and kinetic energy is ultimately converted into radiation and lost to the system (e.g., Mihos & Hernquist 1996; Di Matteo et al. 2007; Cox et al. 2008). These processes lead to the inflow of gas, an increase in gas density (either globally or locally), and hence an increase in the star formation rate (Kennicutt 1998).

Li et al. (2007a) have investigated the link between interactions and star formation in the largest sample of galaxies studied to date. They found a strong correlation between the proximity of a near neighbor (closer than 100 kpc) and the average specific star formation rate. This result pertains to the relatively early stages of an eventual merger. Using lopsidedness as a probe would allow us in principal to measure the history of the enhancement in star formation (in an time-averaged sense) all the way through to the post-merger phase. Zaritsky & Rix (1997) exploited this idea, and found a correlation between lopsidedness and excess B -band luminosity emitted by a young stellar population. Rudnick et al. (2000) showed that both recent (the past 1 Gyr) and ongoing star formation are correlated with lopsidedness, and estimated that as much as 10% of stellar mass in typical galaxies can be formed in such events. However, these papers investigated very small samples compared to the Li et al. (2007a) study.

An additional link between lopsidedness and star formation is indicated by the results in Kereš et al. (2005) and Bournaud et al. (2005). The former authors use SPH simulations to conclude that the star formation history of galaxies is primarily regulated by the accretion rate of cold gas, rather than by mergers. The accretion of this cold gas will not occur in a spherically symmetric fashion, and Bournaud et al. (2005) argue that this will lead to long-lived lopsidedness in disk galaxies.

Large samples are crucial to the investigation of the connection between lopsidedness and the recent star formation history. In our recent paper (Reichard et al. 2008, hereafter Paper I) we reported on our analysis of multi-color Sloan Digital Sky Survey (SDSS) images of ~ 25000 low-redshift ($z < 0.06$) galaxies. We confirmed that Lopsidedness in the stellar mass distribution is indeed very common, and quantified its distribution as a function of the principal structural properties of the galaxies. We found that galaxies of lower mass, lower density, and lower concentration are systematically more lopsided. Similarly, Kauffmann et al. (2003a,b) showed that galaxies with lower mass, density, and concentration have younger stellar populations on-average. Taking these results together, the causal connections between star formation, lopsidedness, and other galaxy structural properties are ambiguous. Unraveling this web of mutual correlations requires the careful analysis of a

large and homogeneous sample.

The strong correlation between the stellar mass of a galaxy and the metallicity of its interstellar medium (Tremonti et al. 2004) provides a powerful constraint on the chemical evolution of galaxies and the intergalactic medium (e.g., Dalcanton 2007). If lopsidedness in a galaxy has been recently induced by either a minor merger with a gas-rich low mass companion galaxy or the accretion of cold intergalactic gas, then one signature would be a decrease in the metallicity of the interstellar medium in lopsided galaxies compared to other galaxies of the same mass. This can be tested with a large sample of galaxies.

Interactions and mergers are also believed to be an important mechanism for fueling the formation and growth of a central supermassive black hole. This idea dates back at least to Toomre & Toomre (1972), and is one of the cornerstones of contemporary models that attempt to explain the co-evolution of galaxies and black holes within the context of the hierarchical build-up of structure (e.g., Hopkins et al. 2007; Di Matteo et al. 2007). However, the observational verification of this idea remains insecure. At high-redshift the data are still too sparse to be conclusive, while at low-redshift there have been many past studies that have led to contradictory results. Li et al. (2007b) have undertaken an analysis of the largest low-redshift sample to date, based on 10^5 galaxies in the SDSS. They find a strong link between close companions and star formation, but none between close companions and AGN. One possibility is that the black hole growth occurs only late in a merger, after the companion galaxy has been captured. This idea can be tested using lopsidedness and a similarly large sample since lopsidedness can be used to trace later stages of interaction than that seen in pair studies.

In this study, we use the large data-set described in Paper I to try to understand how lopsidedness may be linked to star formation, metallicity, and the AGN phenomenon. We describe our specific galaxy sample in §2 and summarize our measurements of the structural parameters, star formation indicators, metallicity, and AGN indicators. Next, in §3, we compare the correlations between star formation and structure with an emphasis on separating out the dependence of star formation on lopsidedness versus other galaxy structural properties. Next, in §4 we explore whether the residuals in the mass-metallicity relation correlate with lopsidedness, and test whether this is a fundamental correlation, or only a secondary one induced through a mutual dependence of metallicity and lopsidedness on galaxy structure. Finally, in §5, we compare lopsidedness and the structural and stellar population properties for the host galaxies of AGN, to test for a possible link between interactions/mergers/accretion and the growth of black holes. We discuss the implications of our conclusions in §6.

2. Data

For the convenience of the reader, we briefly summarize the data, our sample selection, and our methodology here. The details are discussed in Paper I. The sample of galaxies was taken from the Sloan Digital Sky Survey (York et al. 2000; Stoughton et al. 2002), a large survey of photometric and spectroscopic data across π sr. of the northern sky. The sample is derived from SDSS Data Release 4 (Adelman-McCarthy et al. 2006). The survey’s dedicated 2.5 m telescope (Gunn et al. 2006) at Apache Point Observatory uses a unique CCD camera (Gunn et al. 1998) and drift-scanning to obtain u -, g -, r -, i -, and z -band photometry (Fukugita et al. 1996; Hogg et al. 2001; Ivezić et al. 2004; Smith et al. 2002; Tucker et al. 2006). The pixel scale is $0''.396/\text{px}$. Fiber spectroscopy is obtained using $3''$ fibers and results in wavelength coverage between 3800–9200 Å at a resolution $R = \lambda/\delta\lambda = 1850 - 2200$.

Lopsidedness is defined here as the radially averaged amplitude of the $m = 1$ azimuthal Fourier mode between the radii in the SDSS images enclosing 50% and 90% of the galaxy light (R_{50} and R_{90} respectively). In Paper I we showed that galaxies on-average exhibit virtually identical distributions of r - and i -band lopsidedness (and only slightly larger values in the g -band). We showed that weakness of the color dependence of lopsidedness implied that lopsidedness primarily traces the asymmetry in the underlying stellar mass distribution. Since any spatial variations in mass-to-light ratio will be smaller at longer wavelengths, we use the i -band lopsidedness A_1^i throughout this paper.

The calculation of lopsidedness is subject to a handful of observational systematic errors. Insufficient spatial resolution, low signal-to-noise, and highly inclined galaxies in images lead to systematically incorrect measurements of A_1 . Galaxies subjected to these systematic effects were eliminated by requiring the following observational properties: $z < 0.06$, $2R_{50}/(\text{PSF FWHM}) > 4$, total $S/N > 30$ in the region between R_{50} and R_{90} , and $b/a > 0.4$. These restrictions yield a sample of 25155 galaxies that we use in our analysis below. These systematic effects prevent a reliable determination of lopsidedness in the central region of the galaxies (where the star formation properties are calculated). However, it has been shown that the lopsidedness in mergers is very high in the central as well as the outer regions (Jog & Maybhate 2006).

We make extensive use of other galaxy structural parameters derived from the SDSS data (see Kauffmann et al. 2003a). The galaxy stellar mass (M_*) is derived from the SDSS z -band luminosity and a mass-to-light ratio derived from the spectra. The stellar surface mass density μ_* is defined as the mean value within the galaxy half-light radius ($\mu_* = M_*/2\pi R_{50}^2$). We also use the galaxy stellar velocity dispersion σ_* , and the concentration parameter $C = R_{90}/R_{50}$ (the latter serving as a rough proxy for Hubble Type, increasing from ~ 2 for late type galaxies to ~ 3 for early types).

Most of the quantities we use to characterize the properties of the stars, ionized gas, and the AGN are based on the SDSS spectra. The SDSS fiber diameter is $3''$, which for our redshift-limited sample corresponds to a typical projected diameter of about 3 kpc. Our measures of lopsidedness are made using the annulus between the radii enclosing 50% and 90% of the light, a region lying entirely outside the SDSS fiber. *Thus, it is important to emphasize that we are essentially relating the lopsidedness of the outer part of the galaxy to the central properties of the galaxy.*

We use a variety of measurements to provide information about the star formation history in this central region (Kauffmann et al. 2003a). The 4000 Å break, D_{4000} , indicates the current luminosity-weighted mean stellar age. Young stellar populations produce almost no metal absorption just shortward of 4000 Å, giving $D_{4000} \sim 1$, while older populations have strong metal line absorption, and D_{4000} increases to ~ 2 for an age of $\sim 10^{10}$ years. We use the narrow definition of D_{4000} as defined by Bruzual (1983): the ratio of the flux density F_ν in the ranges 4050–4250 and 3750–3950 Å. Reddening affects this narrow definition less than other, wider definitions.

The H δ absorption-line index $H\delta_A$ reaches maximum strength in a simple stellar population with an age of 0.1-1 Gyr when A-stars dominate the continuum. We use the $H\delta_A$ index as defined by Worthey & Ottaviani (1997) where an equivalent width is calculated between two pseudocontinuum bandpasses. The combination of D_{4000} and $H\delta_A$ allows us to recognize objects that have undergone bursts of star formation within the past Gyr (galaxies having abnormally strong $H\delta_A$ for their value of D_{4000}).

Recently, Wild et al. (2007) have applied the methodology of Principal Component Analysis to the near-UV spectral region using synthetic spectra derived from a large library of star formation histories. The amplitudes of the first two principal components correspond closely to higher signal-to-noise measurements of D_{4000} (PC_1 : mean age) and the excess in $H\delta_A$ for a given D_{4000} (PC_2 : a post-burst parameter). We use these parameters in our paper.¹

We also use the specific SFR ($SSFR$ or SFR/M_* : the star formation rate per solar mass of stars in the galaxy) as computed by Brinchmann et al. (2004) based on the nebular emission-lines. Note that this is essentially an instantaneous measure of the central star formation rate (averaged over $\sim 10^7$ years), and is hence complementary to the indicators above which have much longer time-constants.

¹This definition of post-starburst is made without regards to the emission-line properties (unlike some other common definitions). This definition allows the inclusion of both AGN and post-starbursts with some residual star-formation.

As we do not have direct measurements of the *global* stellar ages, we use the age-sensitive Petrosian $g - i$ color from the SDSS images K-corrected to a redshift $z = 0.1$. This approach has the disadvantage that the color can be affected by dust extinction as well as by the mean stellar age.

Type 2 (obscured) AGN are recognized and characterized in the SDSS sample using the methodology in Kauffmann et al. (2003c) and Heckman et al. (2004). This is based on the detection of the signature of the narrow emission-lines that are excited by the AGN. The extinction-corrected luminosity of the [O III] λ 5007 emission-line is taken as an indicator of the AGN bolometric luminosity and black hole accretion rate (see Wild et al. 2007 for a discussion of the extinction correction). The AGN hosts are early-type galaxies with a significant bulge component (Kauffmann et al. 2003c), and so the black hole mass (M_{BH}) is estimated from σ_* assuming the relation determined for bulges in Tremaine et al. (2002). As discussed by Kauffmann et al. (2003c), for Type 2 AGN the SDSS images and spectra are dominated by starlight and so the properties of the host galaxies can be measured in the same way as for non-AGN. The exception is that because the AGN contaminate the nebular emission-lines, the adopted SSFR in these cases is taken from Brinchmann et al. (2004) based on the mean relation between D_{4000} and SSFR measured for non-AGN.

The gas-phase metallicities for the star forming galaxies (non-AGN) are determined from fitting an extensive library of model galaxy spectra to the strong nebular emission-lines (see Tremonti et al. 2004 for details).

3. Star Formation History and Lopsidedness

Our plan for this section is to start with the simplest measures of the relationship between the star formation history and lopsidedness. However, since both lopsidedness (Paper I) and star formation history (Kauffmann et al. 2003b; Brinchmann et al. 2004) correlate separately with other galaxy structural properties, we follow this with a more sophisticated multivariate approach.

3.1. Simple Correlations with Star Formation History

We begin with the Petrosian $g - i$ color of the entire galaxy. In Fig. 1 there is a clear trend of increasing lopsidedness with bluer $g - i$ color, with the median lopsidedness rising from 0.05 to 0.25 as $g - i$ drops from 1.4 to 0.1. This correlation establishes that there is a strong connection between the lopsidedness in the outer region of the galaxy, and the star

formation history of the galaxy on global scales (as shown by Rudnick et al. 2000). In a future paper we will use GALEX plus SDSS photometry to relate lopsidedness to the global star-formation rate.

In the present paper our emphasis is on the central properties of our galaxies, so we now turn to stellar age indicators measured within the fiber. Each of our measures has a somewhat different time dependence. We consider them first individually and then together.

We plot the distribution of A_1^i against D_{4000} in the upper right panel of Fig. 1. Kauffmann et al. (2003b) showed that the local galaxy population is bimodal in the distribution of D_{4000} , dividing into young, late-type galaxies ($D_{4000} < 1.5$) and old early-type galaxies ($D_{4000} > 1.7$). For the young galaxies, the lopsidedness increases strongly with decreasing age: the median rises from 0.1 (mildly lopsided) at $D_{4000} = 1.5$ to over 0.3 (strongly lopsided) at $D_{4000} \sim 1$. Values this low for D_{4000} correspond to extremely young stellar populations (strong starbursts, younger than a few tens of Myr). Most older galaxies ($D_{4000} > 1.7$) uniformly have rather small values of $A_1^i < 0.1$.

In the lower left panel of Fig. 1, we plot the lopsidedness distribution as a function of $H\delta_A$. There is a correlation between median A_1^i and $H\delta_A$ for nearly the entire range of $H\delta_A$, with the median value for A_1^i rising from near 0.05 at $H\delta_A = -1$ to 0.20 at $H\delta_A = 9$. Because values of $H\delta_A$ higher than about 7 can only originate about 0.1 to 1 Gyr after a strong burst of star-formation, we can connect such post-starbursts to events that have produced significant perturbations to the stellar mass distribution.

In the lower right panel of Fig. 1, we show the distribution of lopsidedness as a function of the specific star formation rate (SSFR). Above $\text{SSFR} \sim 10^{-11} \text{ year}^{-1}$ (or below a mass-doubling time of $M_*/\text{SFR} = 10^2 \text{ Gyr}$), there is a strong correlation between star formation and lopsidedness. Typical star-forming galaxies with $\text{SSFR} \sim 10^{-11}$ to $\sim 10^{-10} \text{ year}^{-1}$ are mildly lopsided (median value of about 0.1) while strong starbursts ($\text{SSFR} \sim 10^{-9} \text{ year}^{-1}$) are very lopsided ($A_1^i > 0.2$). The smallest SSFR that can be reliably measured from the spectra is about $10^{-12} \text{ year}^{-1}$. Such galaxies are almost uniformly symmetrical (median $A_1^i \sim 0.05$).

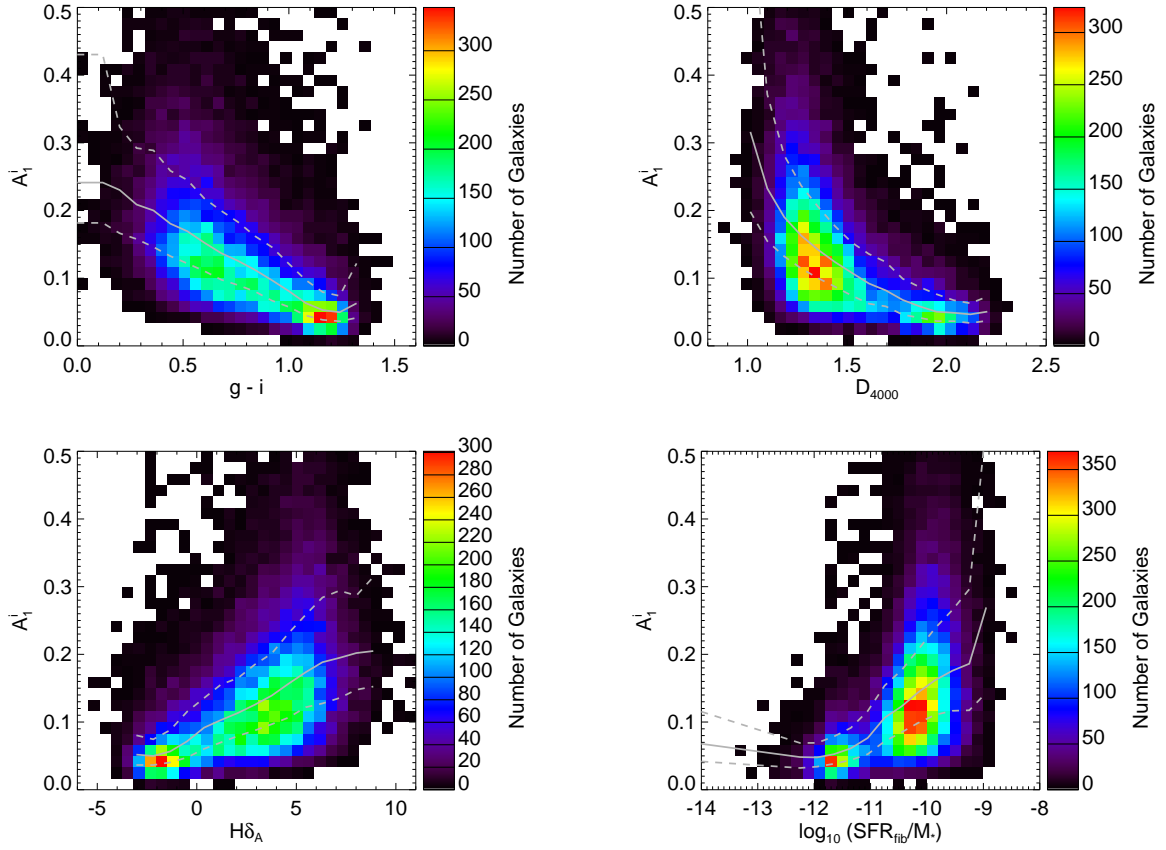


Fig. 1.— Two-dimensional distributions of A_1^i and star formation properties: $g - i$ color, 4000 Å break, $H\delta$ absorption index, and specific star formation rate. The distributions of lopsidedness as functions of these properties are overlaid in gray: median (*solid line*) and quartiles (*dashed lines*). Lopsidedness tends to increase with bluer color, younger stellar population, and higher SSFR.

To orient the reader, in Fig. 2 we show a montage of galaxies selected to cover the range in mass and lopsidedness spanned by our sample of star-forming galaxies. The lopsided galaxies shown ($A_1^i \leq 0.23$) are not extremely distorted like classical major mergers.

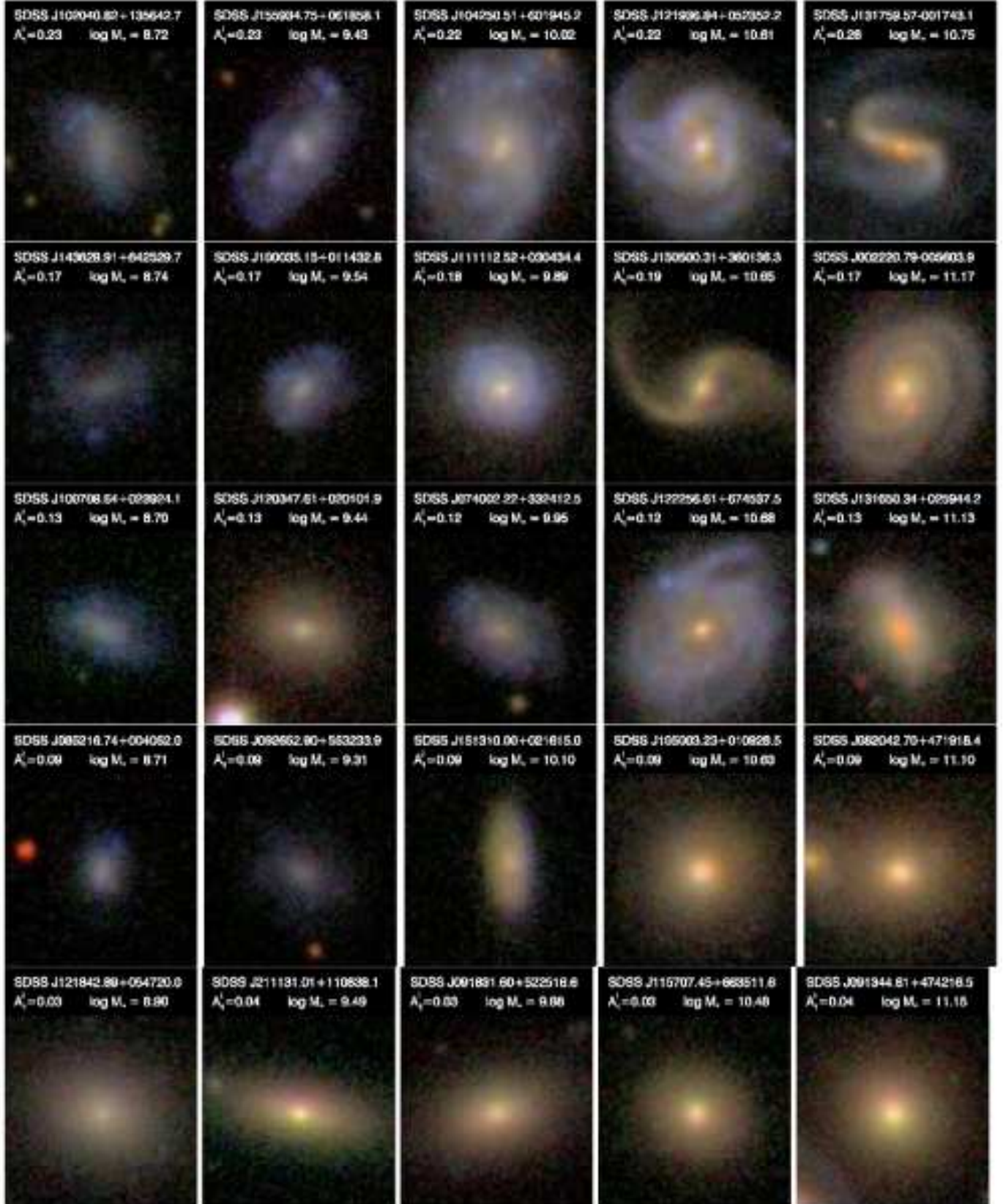


Fig. 2.— Twenty-five SDSS galaxies with increasing lopsidedness from bottom to top and increasing stellar mass from left to right. Each image is $30'' \times 30''$, or about $23 \text{ kpc} \times 23 \text{ kpc}$

As noted above, the two age indicators D_{4000} and $H\delta_A$ used together can identify those galaxies that have undergone a recent ($< \text{Gyr}$) starburst, and separate them from the more common galaxies experiencing more-or-less continuous star formation (Kauffmann et al. 2003a). The parameters PC_1 and $PC_2 - PC_1$ from Wild et al. (2007) provide similar information at higher signal-to-noise. In Fig. 3, we examine the joint dependence of lopsidedness on both D_{4000} and $H\delta_A$ in the left panel and on PC_1 and $PC_2 - PC_1$ in the right. These panels both show that while the main correlation with lopsidedness is between the overall luminosity-weighted mean age (D_{4000} or PC_1), there is also a weaker trend for bursty galaxies at fixed mean age to be more lopsided. This trend can be seen in both plots, as the regions color-coded by median lopsidedness slant from lower left to upper right (implying increasing lopsidedness with the increasing strength of the post-burst signature for a fixed mean age). This result is confirmed in Table 1 where we list the correlation coefficient of lopsidedness with PC_2 , and also the partial correlation coefficient for the residual dependence of lopsidedness on $H\delta_A$ after removing the mutual dependence on D_{4000} . The sample size is sufficient to give these correlations a large statistical significance.

The highest mean values of lopsidedness ($A_1^i > 0.2$) are found along the far left edge of these panels. This region lies along the locus of a starburst evolving to a post-starburst descendant over a period of about 100 Myr (Wild et al. 2007). Galaxies in the region occupied by older post-starbursts (100 Myr to 1 Gyr) are significantly less lopsided ($A_1^i \sim 0.1$ to 0.2). This is reasonable, given that the characteristic dynamical time over which the galaxy should relax after a merger or tidal perturbation is a few hundred Myr. Indeed, the minor merger calculations of Bournaud et al. (2005) show that values for lopsidedness as high as ~ 0.2 last for only a few hundred Myr.

These results are qualitatively consistent with those in Wild et al. (2007) who investigated a sample of relatively massive, bulge-dominated SDSS galaxies (required to have $\mu_* > 10^{8.5} M_\odot/\text{kpc}^2$ and $\sigma_* > 70 \text{ km s}^{-1}$). They also showed that the largest average values of lopsidedness are found in galaxies lying along the locus of starbursts/post-starbursts younger than about 100 Myr. However, the average value of lopsidedness they found for objects lying along this locus was only about 60% as large as what we find in the same region of Figure 3 for our sample. Since we make no cut on μ_* or M_* , this difference is presumably related to the strong inverse correlations we found in Paper I between A_1^i and both μ_* and M_* .

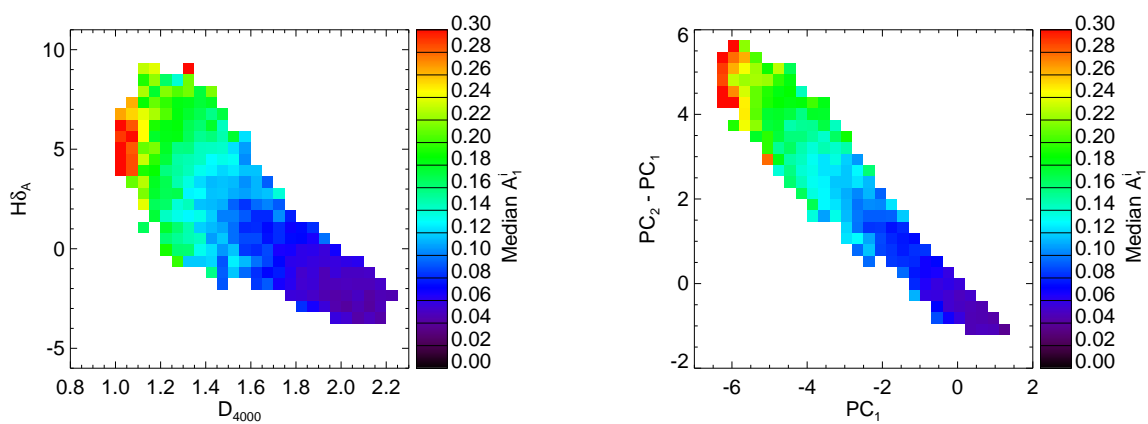


Fig. 3.— Median lopsidedness as a function of the star formation indicators and principal spectral components. Starburst and post-starburst galaxies are typically the most lopsided, while galaxies with little star formation are typically the most symmetric.

3.2. Star-Formation History: Lopsidedness vs. Other Structural Properties

We have shown above that there is a clear correlation between lopsidedness and all our indicators of the star formation history of galaxies. However, in order to establish a true causal connection it is necessary to demonstrate that this correlation is not simply induced by the known strong correlations of the basic galaxy structural parameters (mass, density, and concentration) with both star formation history (Kauffmann et al. 2003b) and with lopsidedness (Paper I).

We begin our assessment of the interdependence between lopsidedness, star formation history, and galaxy structure in Fig. 4. In the three left panels we show the joint dependence of the median value of the age parameter D_{4000} on lopsidedness and each of the three structural parameters. To get a complementary view, the three panels in the right column show the joint dependence of the median A_1^i as a function of D_{4000} and the three structural parameters. The analogous relations using the post-burst diagnostic $PC_2 - PC_1$ and SSFR are shown in Fig. 5 and Fig. 6. These figures refer to the star formation history in the central region of the galaxy (inside the fiber). In Figure 7 we show the same set of plots, but now using the Petrosian $g - i$ color as an indicator of the global star formation history of the galaxy. Our result is similar to Woods & Geller (2007) who find that the star formation becomes more centrally concentrated in interacting galaxies as the pair separation decreases and the specific star formation rate increases.

In all the plots the overall trends are broadly similar: the left-hand panels show that galaxies with larger values of lopsidedness and smaller values of mass, density, and concentration have younger stellar populations.² In each case, for a fixed value of a structural property (mass, density, or concentration), the stellar population becomes younger as the lopsidedness increases. Pictorially, we see that the bands color-coding the stellar age have diagonal or horizontal orientations. Similarly, the right hand panels in all three figures show that galaxies with younger stellar populations and lower masses, densities, and concentrations are more lopsided. In each case, for a fixed value of a structural property (mass, density, or concentration), the galaxies become more lopsided as the stellar population becomes younger: again, we see that the bands color-coding the lopsidedness have a diagonal or horizontal orientation.

We conclude from this that there is a correlation between lopsidedness and the star

²In the left hand panels of Fig. 6 we are unable to calculate a meaningful value for the median SSFR for galaxies lying in the region of low lopsidedness and high mass, density, or concentration. This is because the SSFR in most galaxies is too small to be reliably measured. We leave this region blank, but the low median SSFRs there ($\leq 10^{-12}$ year⁻¹) are consistent with what is seen in the figures using the other age indicators

formation history that is independent of any mutual correlation on the other galaxy structural parameters. To quantify this result, we turn to a partial correlation analysis to reveal which correlations are the strongest and perhaps the most fundamental. Table 1 shows the correlation coefficients of various combinations of structural and star formation properties. Values of $\log_{10} SFR/M_*$ below -12 have been set to -12 (see above). The results in this table show that there are separate and significant correlations between the structural properties themselves (independent of lopsidedness or star formation history), between lopsidedness and the other structural parameters (independent of star formation history), and between star formation history and lopsidedness (independent of the other structural parameters). These results are fully consistent with the visual representations in the figures.

The lower left panels in both Figures 5 and 6 show that the relatively symmetric galaxies with $A_1^i < 0.15$ have higher values of $PC_2 - PC_1$ and SSFR for less concentrated galaxies. However, the trend is reversed for the highly lopsided galaxies with $A_1^i > 0.2$. These lopsided galaxies typically show higher SSFR and larger $PC_2 - PC_1$ at higher concentration. The most natural interpretation is that these are objects that are undergoing or have recently undergone central starbursts (leading to an increased concentration of light). This is consistent with the fact that an analogous behavior is not clearly seen in Figure 7 where we are investigating the *global* star formation history using the Petrosian $g - i$ color. Here, the youngest (bluest) galaxies are lopsided but have low concentration.

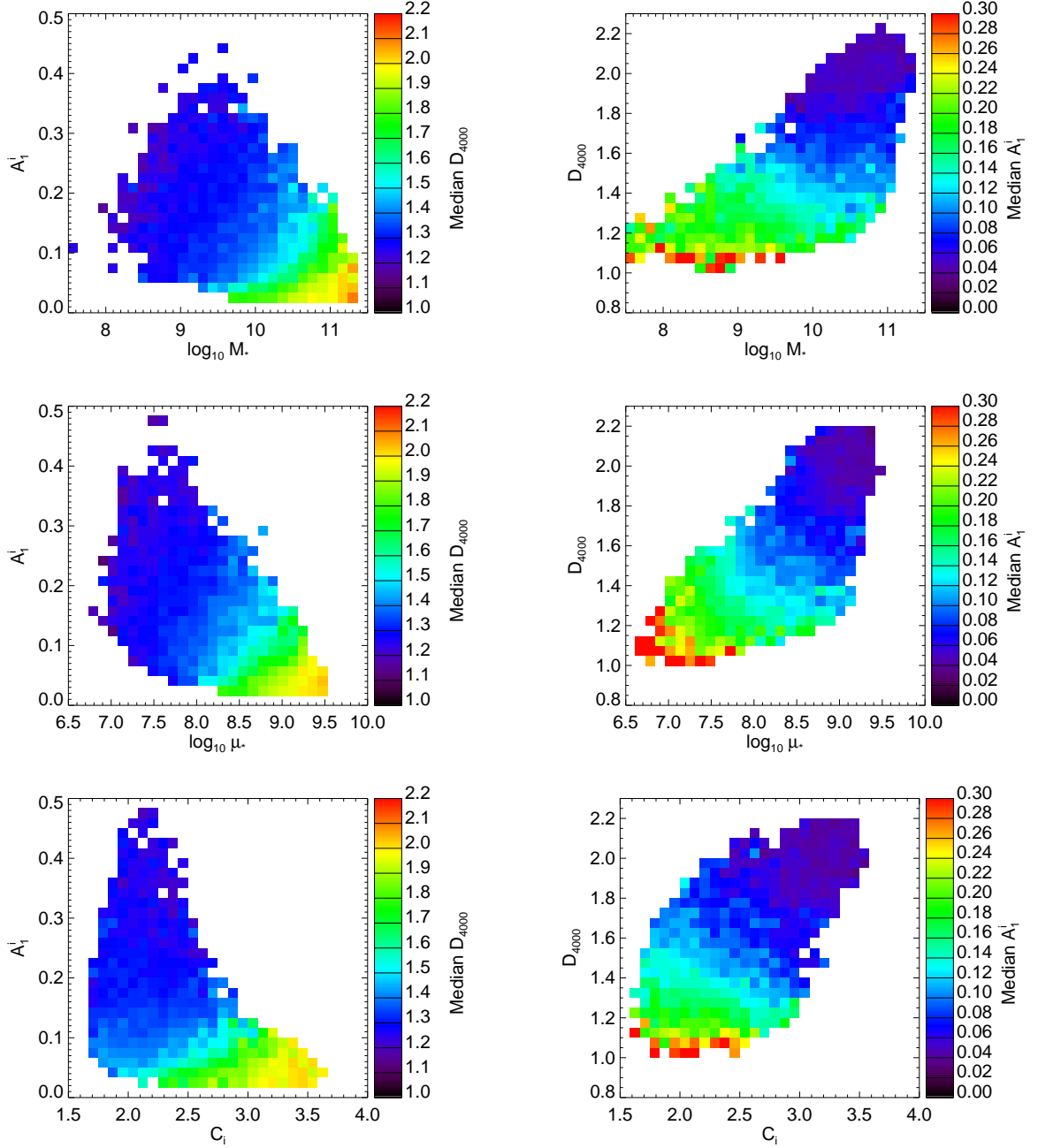


Fig. 4.— Relationships between stellar age and structure shown in several slices of this parameter space. The color-coding of these two-dimensional histograms indicates the median D_{4000} or A_1^i . Galaxies with higher lopsidedness and smaller values of the other structural properties tend to have younger stellar populations.

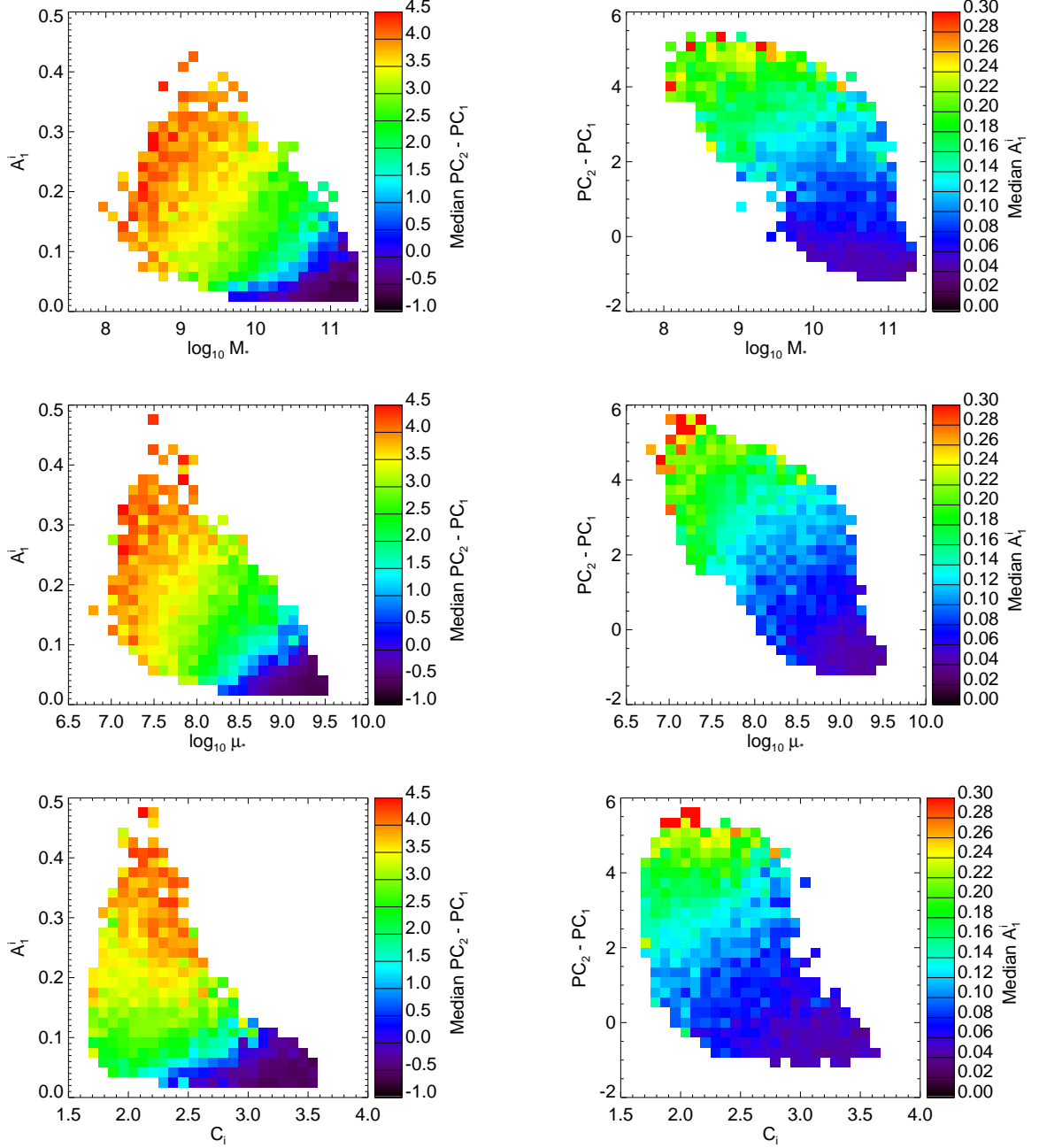


Fig. 5.— Relationships between $PC_2 - PC_1$ and structure shown in several slices of this parameter space. The color-coding of these two-dimensional histograms indicates the median $PC_2 - PC_1$ or A_1^i . Galaxies with higher lopsidedness and smaller values of the other structural properties tend to have greater values of $PC_2 - PC_1$ and thus indicate recent star formation.

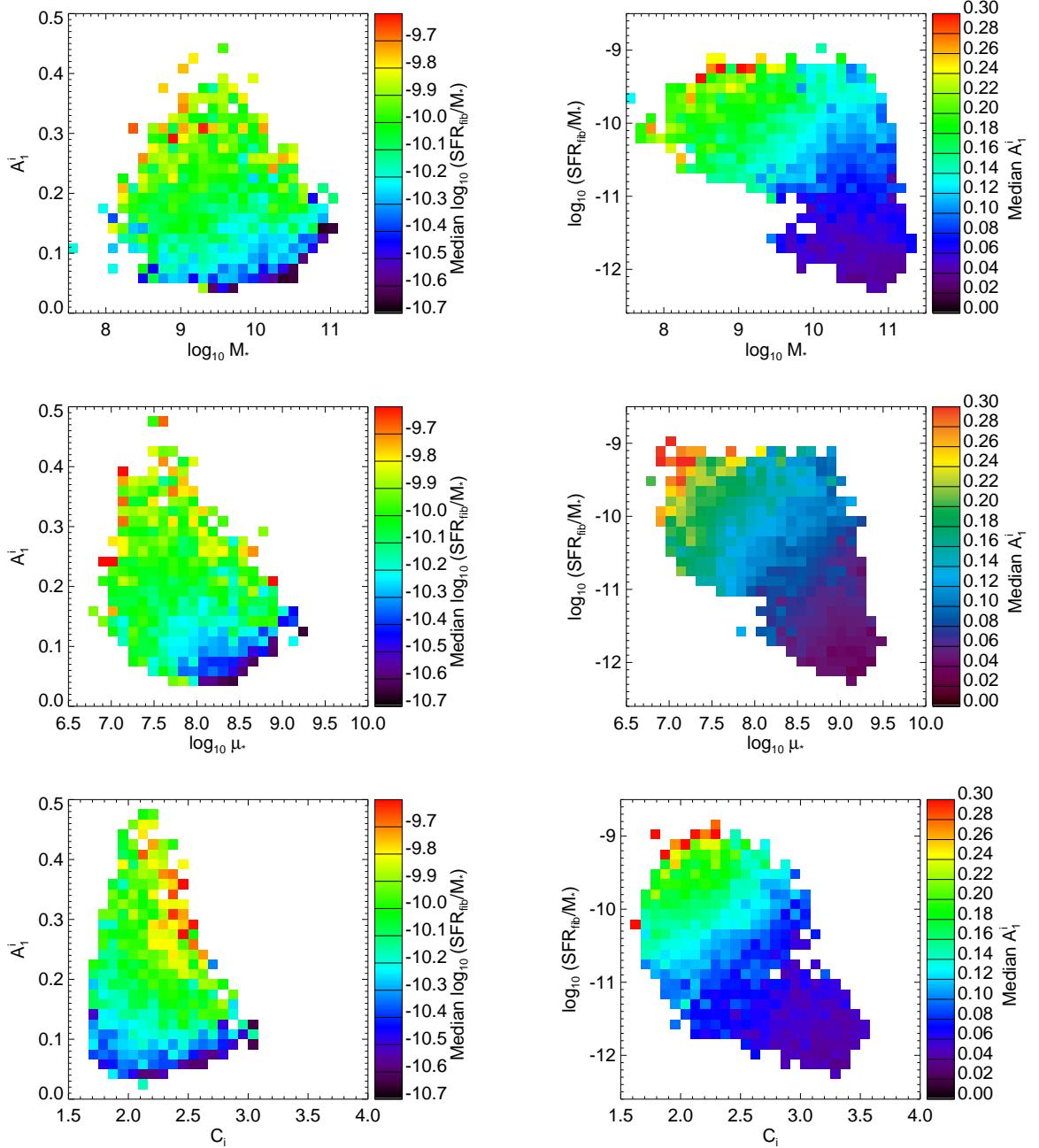


Fig. 6.— Relationships between specific SFR and structure shown in several slices of this parameter space. The color-coding of these two-dimensional histograms indicates the median SSFR or A_1^i . Galaxies with higher lopsidedness and smaller values of the other structural properties tend to have higher SSFR, though the relationship with concentration is more complex.

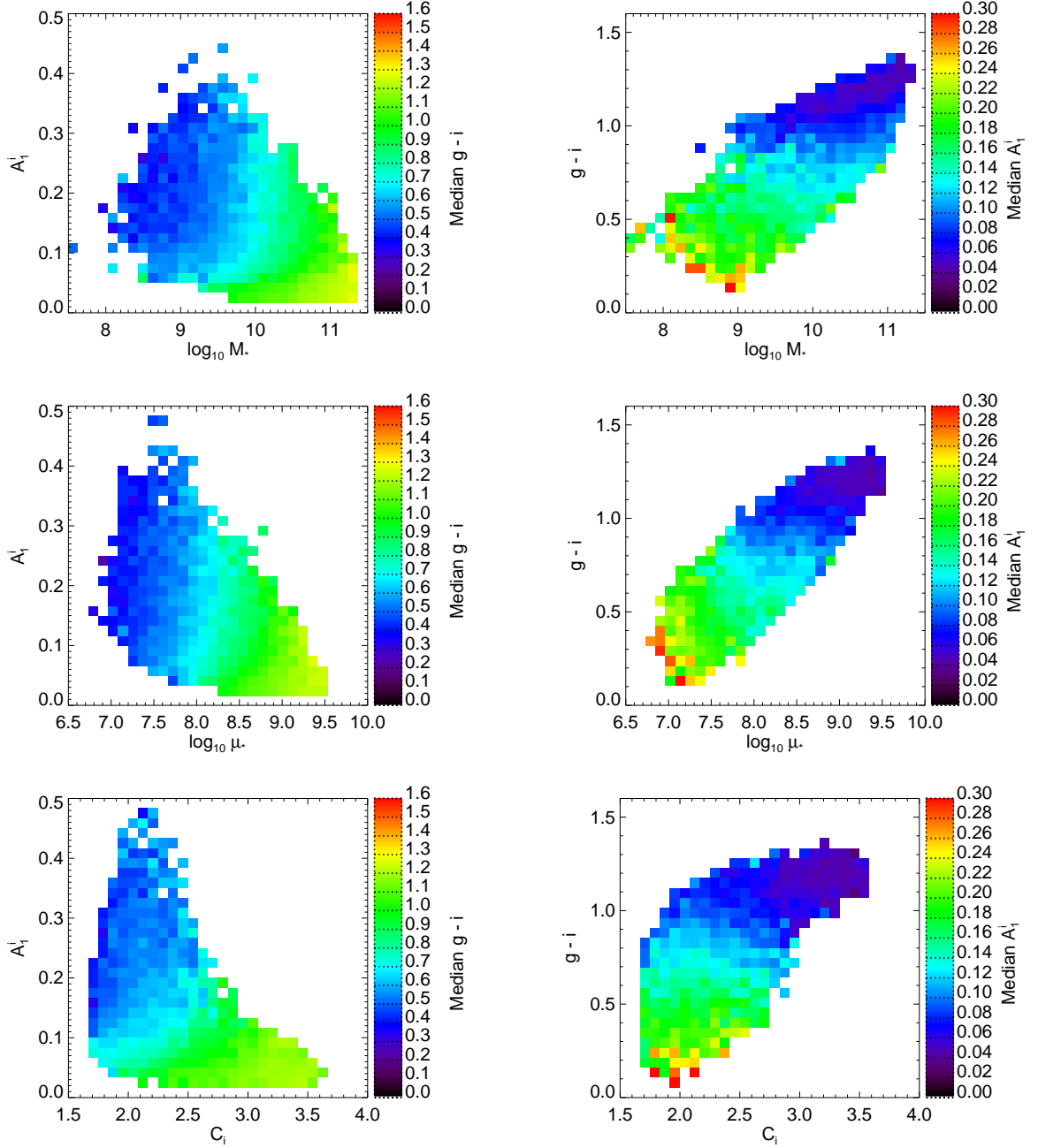


Fig. 7.— Relationships between $g - i$ color and structure shown in several slices of this parameter space. The color-coding of these two-dimensional histograms indicates the median $g - i$ or A_1^i . Galaxies with higher lopsidedness and smaller values of the other structural properties tend to have bluer colors.

4. Metallicity and Lopsidedness

The results above suggest that the processes that produce lopsidedness lead to an inflow of gas into the central region where it can fuel star formation. Any plausible source for this gas (capture of a small galaxy, gas transported from the outer disk to the inner region, the accretion of intergalactic gas) will have a lower metallicity than the pre-existing gas in the central region. Thus - provided that the inflow is rapid enough that the gas is not fully enriched by associated star formation before reaching the center - this inflow should have a signature in the chemical abundances in the interstellar medium. This has been seen by Kewley et al. (2006) and by Ellison et al. (2008a) for interacting galaxy pairs. Such a signature would also be consistent with Ellison et al. (2008b) who found that residuals in the mass-metallicity relation correlate inversely with the specific star formation rate.

To test this idea, in Figure 4, we show the mass-metallicity relation for our sample, color-coded by the median value for the lopsidedness in each cell. The strongest trend in this figure is simply the increase in lopsidedness with decreasing galaxy mass (Paper I). However, there is a weaker residual trend for the lopsidedness at a given value of stellar mass to increase with decreasing metallicity. This can also be seen in Table 2 where we list the relevant partial correlation coefficients.

Tremonti et al. (2004) showed that residuals in the mass-metallicity relation correlate with the surface mass density (with lower metallicity at fixed mass for less dense galaxies). We saw in Paper I that there is a strong inverse correlation between surface mass density and lopsidedness. Could the apparent correlation between lopsidedness and metallicity in Figure 4 be induced through mutual correlations with surface density? The lower panel in Figure 4 shows that at fixed surface mass density galaxies that have lower metallicity are more lopsided. This is confirmed by the partial correlation coefficients in Table 2. We therefore conclude that there is real correlation between lopsidedness and metallicity in the sense expected for an inflow of lower metallicity gas.

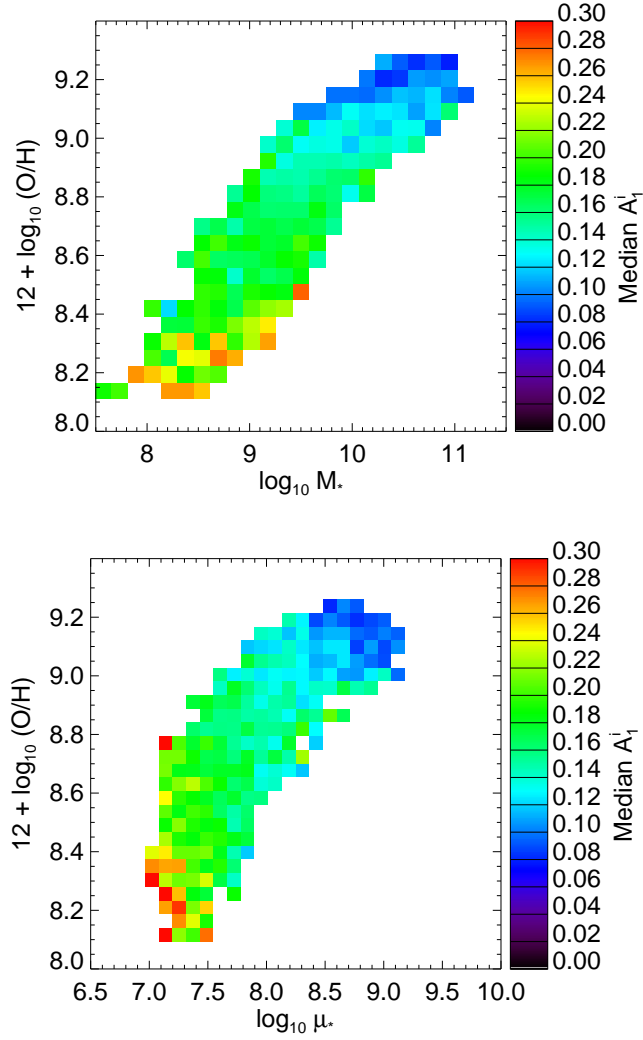


Fig. 8.— Relationships between metallicity and structure shown in two slices of this parameter space. The color-coding of these two-dimensional histograms indicates the median A_1^i . While the main correlation between the three parameters is between lopsidedness and either other structural parameter, there is a residual correlation between lopsidedness and metallicity at fixed mass.

We finish this section by quantifying the metallicity deficit between the most and least lopsided galaxies of our sample. We use two subsamples taken from our main sample: low-lopsidedness galaxies ($A_1^i < 0.08$) and high-lopsidedness galaxies ($A_1^i > 0.20$). We compare the mass-metallicity relations of the two subsamples in Fig. 4. The median metallicity of the less lopsided galaxies is 0.05–0.15 dex greater than in the more lopsided galaxies at the same mass. The metallicity difference is greater at low mass than at high mass. This deficit is consistent with the offset found in Ellison et al. (2008) for galaxies with close companions. The relatively small amplitude of the effect would rule out an extreme picture in which very metal poor gas falls into the center and dominates the interstellar medium there.

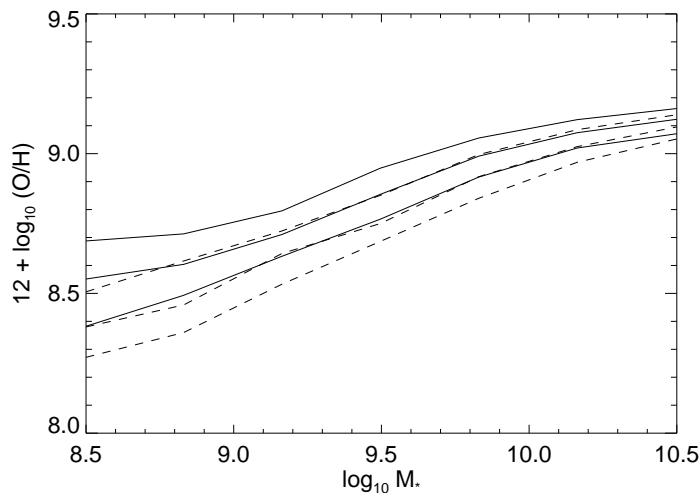


Fig. 9.— Mass-metallicity relation for the most ($A_1^i > 0.2$, *dashed lines*) and least lopsided ($A_1^i < 0.08$, *solid lines*) galaxies. The 25th, 50th, and 75th percentile lines are shown for each distribution. The most lopsided galaxies have a metallicity deficit of 0.05–0.15 dex compared to the least lopsided galaxies at the same mass. The deficit is greater at low mass than at high mass.

5. Nuclear Activity and Lopsidedness

We start with the simplest measures of the relationship between AGN and lopsidedness. However, since both lopsidedness (Paper I) and AGN properties (Kauffmann et al. 2003c; Heckman et al. 2004; Kewley et al. 2006b) correlate separately with other galaxy structural properties, we follow this with a multivariate approach to isolate the specific role of lopsidedness. We also know that AGN with higher luminosity are preferentially located in galaxies with younger central stellar populations (Kauffmann et al. 2003c, 2007), and we have seen above that galaxies show a strong link between lopsidedness and a young central stellar population. We will attempt to sort out this complex web of correlations using an approach based on comparing AGN hosts to “twin” galaxies without AGN that have been matched to the AGN hosts in their structure and central stellar population.

We begin with Figure 10 in which we plot the distribution of lopsidedness in the diagnostic line ratio diagram used by Kauffmann et al. (2003c) to select Type 2 AGN (the “BPT Diagram”, after Baldwin et al. 1981). As discussed in Kauffmann et al. (2003c) and Kewley et al. (2006b), the distribution running from the upper left to the lower right is the locus of star forming galaxies (with low metallicity at the top left and high metallicity at the lower right). The spur running to the upper right off the location of the metal-rich star forming galaxies is the locus of AGN. It represents a “mixing line” with AGN dominated objects at the upper right and star-forming/AGN composite objects at the lower left close to where the AGN spur joins the locus of star forming galaxies.

It is clear from this plot that star forming galaxies are systematically more lopsided than AGN host galaxies. This is not surprising, since Kauffmann et al. (2003c) show that AGN hosts are generically massive, dense galaxies (which we have shown in Paper I to typically have small values for A_1^i). In the region occupied by the AGN the median value of A_1^i is less than 0.1, with a weak trend for lopsidedness to be larger in the composite objects than in the pure AGN. This trend is not surprising, given the connection between lopsidedness and star formation discussed above.

The Type 2 AGN in our sample span a large range in luminosity, and it is quite possible that the mechanism responsible for fueling the growth of the black hole might change systematically as a function of AGN luminosity. To examine this, in Figure 11 we plot the distribution of A_1^i vs. the ratio of the extinction-corrected [O III]5007 emission line luminosity to the black hole mass. This ratio will be roughly proportional to the black hole accretion rate relative to the Eddington limit (see Heckman et al. 2004).

We see in this plot that there is a systematic increase in lopsidedness with increasing AGN luminosity (increasing black hole growth rate). Below values of $L[\text{O III}]/M_{BH} \sim$

$10^{-2}L_{\odot}/M_{\odot}$ (corresponding roughly to accretion rates less than 10^{-4} of the Eddington limit), the median value of A_1^i is only ~ 0.05 (lopsidedness is essentially undetectably small). The median lopsidedness then increases with increasing AGN luminosity, reaching a value of $A_1^i \sim 0.12$ at $L[\text{O III}]/M_{BH} = 10L_{\odot}/M_{\odot}$ ($\sim 10\%$ of the Eddington limit). This median value corresponds to only mild lopsidedness and (even at such high AGN luminosities) only about 10% of the AGN hosts are strongly lopsided ($A_1^i > 0.2$). Thus, few of the high luminosity AGN hosts appear to be undergoing major mergers, but many are mildly disturbed. To give the reader a visual impression of the structure of AGN hosts we show a montage of SDSS color images of low- and high-luminosity AGN in Figure 12.

Figure 11 by itself does not establish a direct connection between AGN luminosity and lopsidedness. As discussed in Kauffmann et al. (2003c) and Kewley et al. (2006b), the properties of AGN hosts vary systematically as a function of AGN luminosity, and we have seen that lopsidedness is in turn strongly linked to galaxy structural properties (Paper I). Thus, in Figure 13 we examine the interdependence between lopsidedness, galaxy structure, and AGN luminosity. In the left three panels we see that, at fixed galaxy mass, density, and concentration, the median AGN luminosity increases with increasing lopsidedness. Similarly, the right-hand panels show that at fixed values of galaxy mass, density, and concentration the median value of lopsidedness increases with increasing AGN luminosity. The trends are most clear in the panels involving mass, and least clear in those involving concentration. These results are confirmed by the partial correlation coefficients listed in Table 3.

We conclude that there is a link between AGN luminosity and lopsidedness that is independent of the other galaxy structural parameters. This is analogous to the results for star formation, but the trends for the AGN are significantly weaker (the range spanned by the variation in the median lopsidedness in the AGN hosts is much smaller than in the star forming galaxies).

The age of the stellar population in AGN host galaxies decreases systematically as a function of increasing AGN luminosity Kauffmann et al. (2003c, 2007). We have also seen above that there is a very strong inverse correlation between lopsidedness and stellar age. Is the trend for more powerful AGN to be hosted by galaxies that are more lopsided simply induced by these other correlations? One way to visualize this is to plot the joint dependence of AGN luminosity on both stellar age (D_{4000}) and lopsidedness. This is shown in Figure 14. We see clearly that the primary correlation is that between the age of the stellar population and AGN luminosity with little dependence on lopsidedness (the color-coded bands of AGN luminosity are nearly horizontal). This is further quantified by the correlation coefficients in Table 3.

A more direct way to ask the question is as follows: for fixed values of both galaxy

structural and stellar age parameters, is there a remaining trend for higher luminosity AGN to be hosted by more lopsided galaxies? The large number of parametric dimensions involved in such a test leads us to adopt a “twinning” strategy. That is, for each AGN with a given value of $L[\text{O III}]/M_{BH}$ we will find within our sample another non-AGN galaxy with the same redshift, stellar mass, surface mass density, and stellar age (same value of D_{4000}). The matching tolerances in redshift, mass, surface mass density, and D_{4000} were 0.005, 0.05 dex, 0.05 dex, and 0.10, respectively.

In Figure 15, we compare the distributions of lopsidedness as a function of the AGN luminosity for the AGN hosts and their non-AGN twin galaxies. In this plot, we have assigned each non-AGN twin the value for $L[\text{O III}]/M_{BH}$ of its AGN twin. We have also plotted the distribution of the difference in lopsidedness (AGN host minus twin) as a function of AGN luminosity. We see from this figure that there is no systematic difference between the AGN hosts and their twins. We conclude that the trend for more powerful AGN to be hosted by galaxies that are more lopsided is due to the strong link of the age of the stellar population in the galaxy bulge to both the AGN luminosity and to the lopsidedness of the host galaxy. This can also be seen in Figure 16 where we show the very similar dependence between stellar age and lopsidedness for both the AGN hosts and their twins. These results are quantified by the partial correlation coefficients in Table 3.

This leads us to the following thoughts. It is clear that the processes that produce lopsidedness facilitate the delivery of gas into the central regions of galaxies. It is also clear that the presence of cold gas in the central region (however it arrives there) is required for the formation of stars there. The fact that the more rapidly growing black holes are strongly associated with a younger stellar population implies that the presence of cold gas in the central region is also required for rapid fueling of the black hole. The results above then suggest that the once the gas has arrived in the central kpc-scale region, some other process (not directly related to the cause of the lopsidedness) regulates the subsequent transfer of a small fraction of the gas inward by orders-of-magnitude in radius to the black hole accretion disk.

It is interesting to compare our results to those of Li et al. (2007b), who have examined a very similar SDSS galaxy sample for a link between the presence of close companion galaxies and the fueling of black holes. They found that close companions are associated with a significant boost in the star formation rate, but are not associated with an enhancement of nuclear activity (compared to galaxies of similar mass). Ellison et al. (2008a) reached similar conclusions with a different sample drawn from SDSS. These results contrast with our result showing that (at fixed galaxy mass, density, or concentration) higher AGN luminosities are preferentially found in galaxies that are more lopsided.

Li et al. (2007b) concluded from their results that the star formation induced by a close companion and the star formation associated with black hole accretion are distinct events. They argued that these events may be part of the same physical process, for example a merger, provided they are separated in time. They therefore speculated that accretion onto the black hole and its associated star formation occurs after the two interacting galaxies have merged. This scenario is consistent with our results, since lopsidedness will persist for several galaxy dynamical times after the merger is complete. In a future paper we will combine our results on close companions and lopsidedness to try to test this idea.

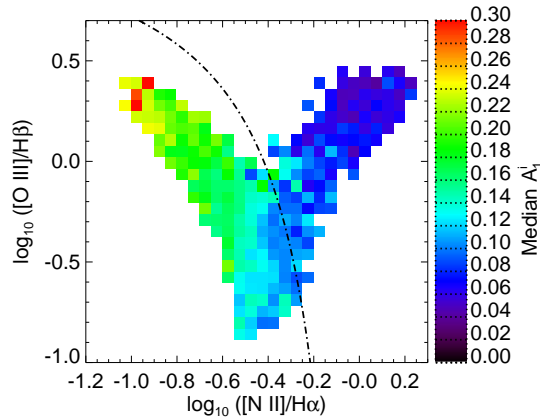


Fig. 10.— BPT diagram color-coded by median A_1^i . The strong correlation with lopsidedness is that with star formation rather than that with AGN activity. The black line separates the AGN from the star-forming galaxies and is adopted from Kauffmann et al. (2003c).

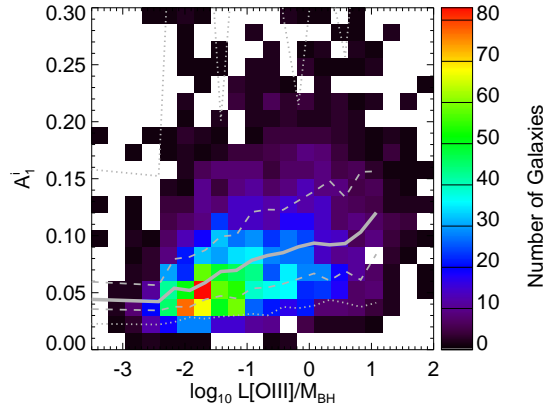


Fig. 11.— The distribution of A_1^i and $L[\text{O III}]/M_{BH}$ for all galaxies in the sample. The 5th, 25th, 50th, 75th, and 95th percentiles of A_1^i are overplotted in gray. Typical lopsidedness increases with $L[\text{O III}]/M_{BH}$. Median A_1^i reaches a moderate value ($A_1^i = 0.1$) when $L[\text{O III}]/M_{BH}$ is high at $10 L_\odot/M_\odot$.

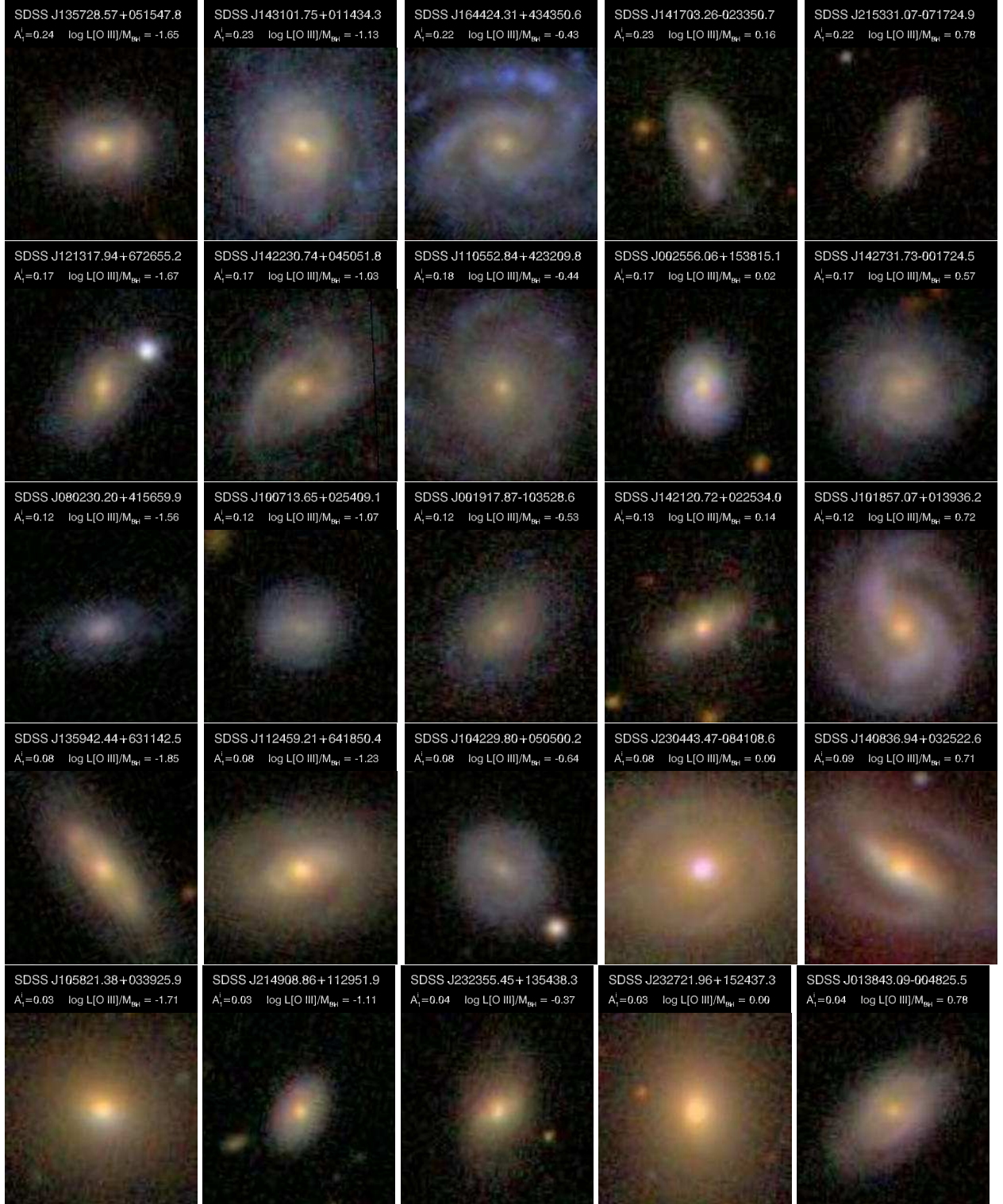


Fig. 12.— Twenty-five SDSS galaxies with increasing lopsidedness from bottom to top and increasing $L[\text{O III}]/M_{\text{BH}}$ from left to right. Each image is $30'' \times 30''$, or about $23 \text{ kpc} \times 23 \text{ kpc}$ at $z = 0.04$, a typical redshift of the sample.

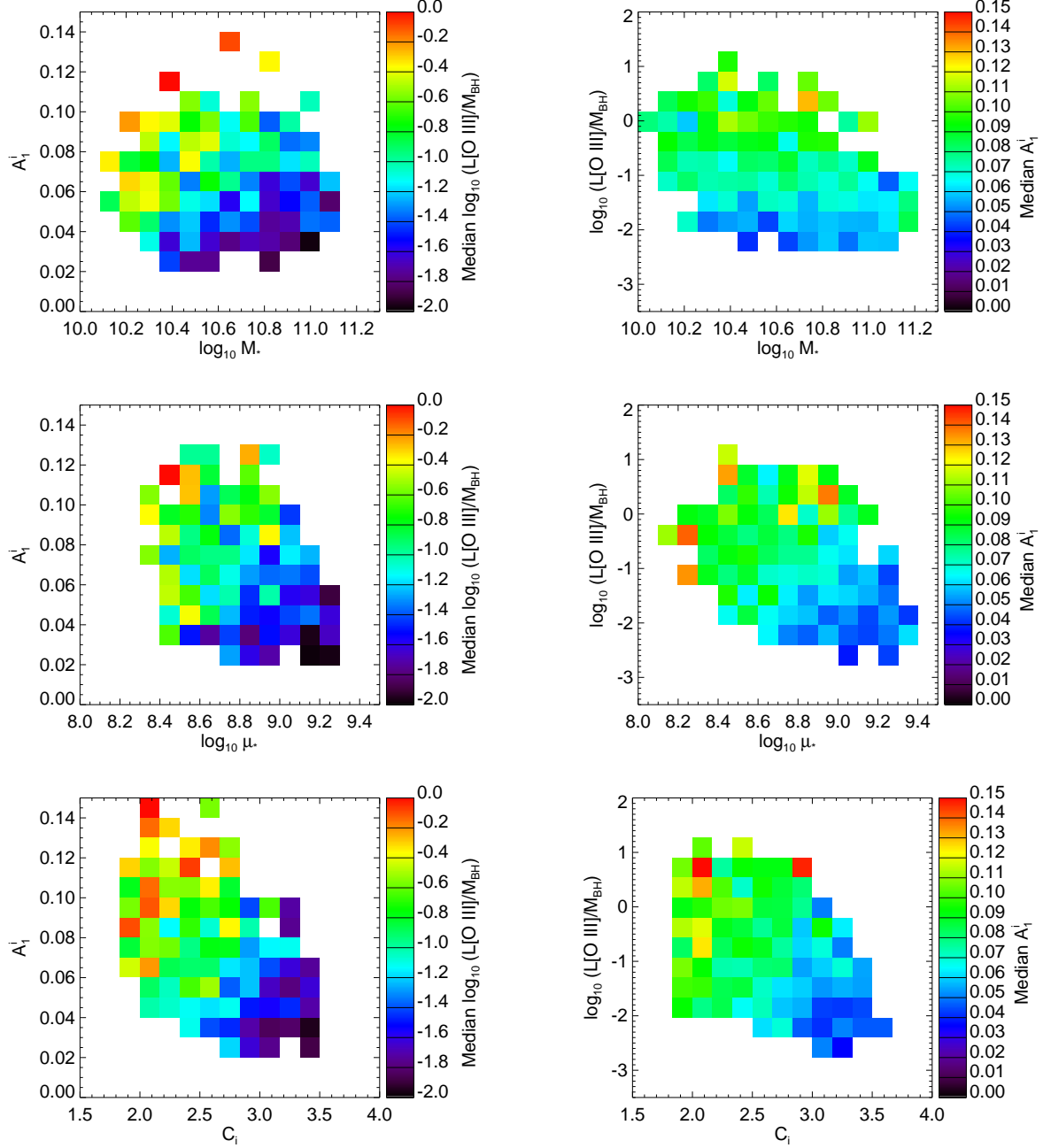


Fig. 13.— Relationships between $\text{L[O III]}/M_{\text{BH}}$ and structure shown in several slices of this parameter space. The color-coding of these two-dimensional histograms indicates the median $\text{L[O III]}/M_{\text{BH}}$ or A_1^i . In each case, there is a correlation between lopsidedness and AGN luminosity independent of these structural parameters.

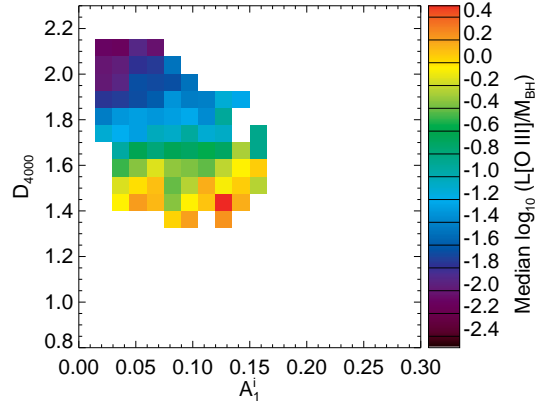


Fig. 14.— Relationship between $L[\text{O III}]/M_{BH}$, D_{4000} , and structure. The color-coding of these two-dimensional histograms indicates the median $L[\text{O III}]/M_{BH}$. The primary correlation is between stellar age and $L[\text{O III}]/M_{BH}$. There is no noticeable correlation between $L[\text{O III}]/M_{BH}$ and lopsidedness in this data.

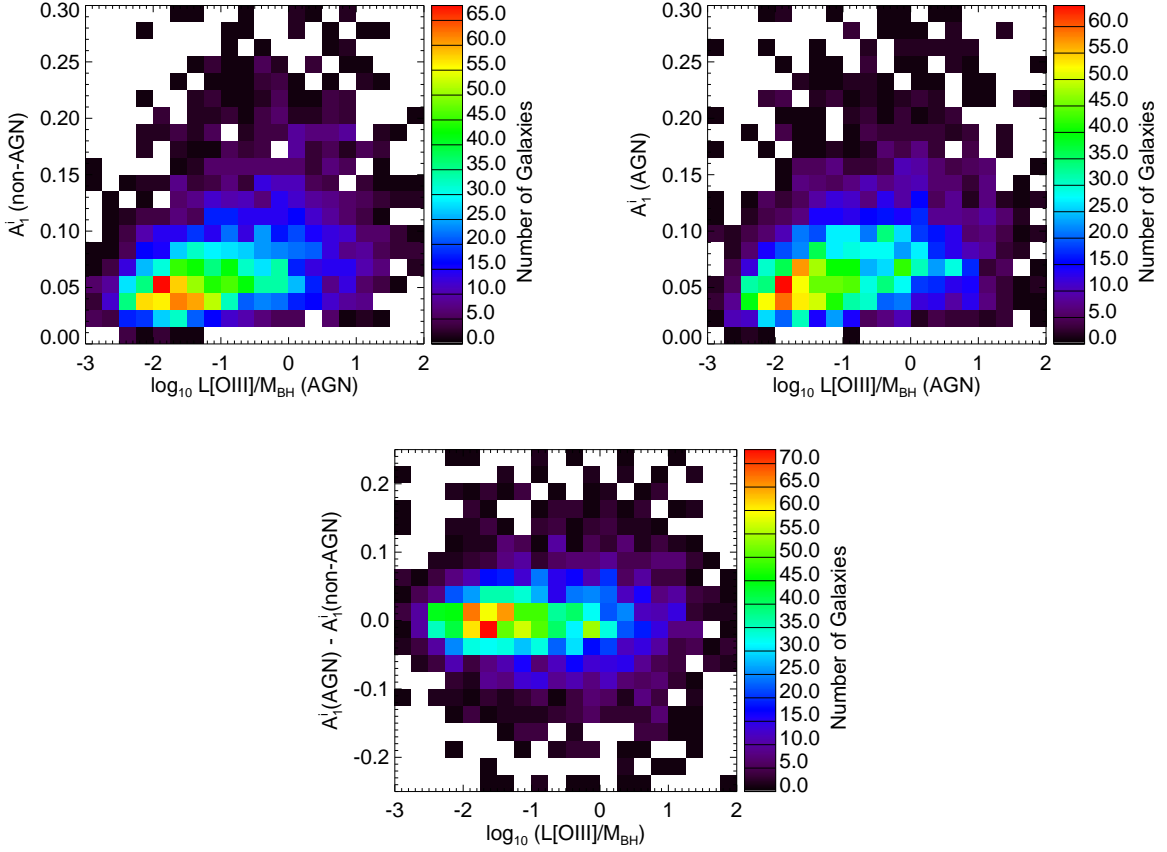


Fig. 15.— *Top left and top right:* Two-dimensional distributions of $L[\text{O III}]/M_{\text{BH}}$ and lopsidedness of non-AGN and AGN galaxy pairs matched in redshift, mass, mass density, and stellar age (D_{4000}). The distributions show no significant difference between the lopsidedness-AGN luminosity relationship. *Bottom:* Difference in lopsidedness of the AGN and non-AGN in matched galaxies pairs vs. the AGN luminosity. No preference is shown for the AGN or non-AGN to be more often more lopsided than the other for any value in our range of $L[\text{O III}]/M_{\text{BH}}$.

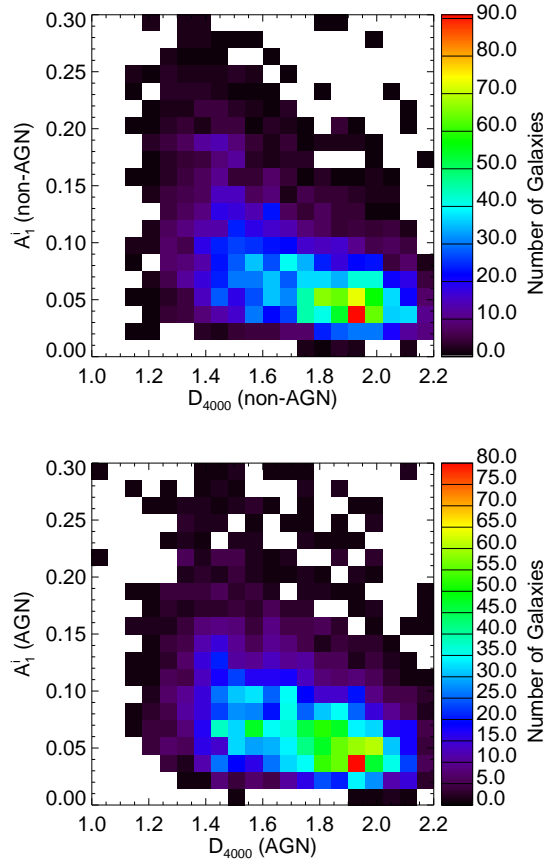


Fig. 16.— Relationship between lopsidedness and mean stellar age (D_{4000}) for the AGN and non-AGN in pairs of galaxies matched in redshift, mass, mass density, and mean stellar age. The star formation-lopsidedness connection is similar for AGN and non-AGN.

6. Summary

We have studied a sample of approximately 25000 low-redshift ($z < 0.06$) galaxies from the Sloan Digital Sky Survey (SDSS) Data Release 4 to investigate the links between large-scale asymmetries in the stellar mass distribution in galaxies (lopsidedness), star formation, the metallicity of the interstellar medium, and the presence of active galactic nuclei (AGN). Lopsidedness has been defined as the radially averaged $m = 1$ azimuthal Fourier amplitude (A_1) measured between the radii enclosing 50% and 90% of the galaxy light in the SDSS images (i.e. in the outer part of the galaxy). We have previously shown that lopsidedness traces the distribution of the underlying stellar mass (Paper I). Lopsidedness is a signpost of a non-equilibrium global dynamical state, and can be induced by mergers, asymmetric accretion of cold gas, tidal interactions, or underlying asymmetries related to the dark matter halo. We have used spectra obtained through the SDSS 3" diameter fibers (typical projected diameter of ~ 3 kpc) to characterize the stars, gas, and AGN in these central regions.

We have used the amplitude of the 4000 Å break, the strength of the high-order Balmer absorption-lines, and the specific star formation rate derived from the nebular emission-line to characterize the stellar population in the central few-kpc-scale region. We found strong links between lopsidedness and recent/on-going central star-formation: galaxies with younger stellar populations are more lopsided and more lopsided galaxies have younger stellar populations. Starburst and post-starburst galaxies are the most lopsided on average.

We have previously shown that galaxies with lower surface mass density and mass are more lopsided (Paper I), and that galaxies with lower mass and lower density have younger stellar populations (Kauffmann et al. 2003b; Brinchmann et al. 2004). Here, we have shown that there is still a strong correlation between lopsidedness and the age of the stellar population even after their mutual dependences on these other structural parameters have been removed. These results are consistent with other evidence that mergers and tidal interactions trigger central star-formation, but place these results on a firm statistical base. They are also consistent with the idea that star formation in galaxies today is regulated by the accretion of cold gas (Kereš et al. 2005) which can excite lopsidedness (Bournaud et al. 2005). They imply that the timescale for the transport of gas into the central region can not be significantly longer than the timescale over which lopsidedness persists in the outer disk. This is consistent with recent numerical simulations of star formation in minor mergers and galaxy interactions (Di Matteo et al. 2007; Cox et al. 2008).

We have also shown that at fixed stellar mass, more lopsided galaxies have systematically lower gas-phase metallicities by about 0.1 dex on average. This suggests that the processes causing lopsidedness deliver lower metallicity gas into the central region, but the small amplitude of the effect rules out extreme events as being typical.

Finally, we found that there is a trend for the more rapidly growing black holes to be hosted by galaxies with higher average lopsidedness. This is true when comparing galaxies at fixed galaxy mass, surface mass density, and concentration. However, when the AGN hosts were compared to non-active galaxies that were also matched in the age of the stellar population in their central region, we found no excess lopsidedness in the AGN hosts. The strongest link is that between the youth of the stellar population and the growth rate of the black hole. The correlations of these two properties with lopsidedness are weaker. This suggests that the presence of cold gas in the central few kpc-scale region (which is facilitated through the processes that produce lopsidedness, and which leads to significant star formation) is a necessary but not sufficient condition for subsequent fueling of the growth of the black hole. Other processes are subsequently required to deliver the gas from scales of a few kpc all the way to the black hole accretion disk and these would not be directly related to the process(es) that produced lopsidedness.

Combining our results with the analysis by Li et al. (2007b) and Ellison et al. (2008a) of the role of close companion galaxies in driving star formation and fueling black holes, suggests that the period of black hole growth may be preferentially associated with the end stages of a minor merger. This idea will be tested in a future paper.

We would like to thank Christy Tremonti for reading a draft of this manuscript. Funding for the SDSS and SDSS-II has been provided by the Alfred P. Sloan Foundation, the Participating Institutions, the National Science Foundation, the U.S. Department of Energy, the National Aeronautics and Space Administration, the Japanese Monbukagakusho, the Max Planck Society, and the Higher Education Funding Council for England. The SDSS Web Site is <http://www.sdss.org/>.

The SDSS is managed by the Astrophysical Research Consortium for the Participating Institutions. The Participating Institutions are the American Museum of Natural History, Astrophysical Institute Potsdam, University of Basel, University of Cambridge, Case Western Reserve University, University of Chicago, Drexel University, Fermilab, the Institute for Advanced Study, the Japan Participation Group, Johns Hopkins University, the Joint Institute for Nuclear Astrophysics, the Kavli Institute for Particle Astrophysics and Cosmology, the Korean Scientist Group, the Chinese Academy of Sciences (LAMOST), Los Alamos National Laboratory, the Max-Planck-Institute for Astronomy (MPIA), the Max-Planck-Institute for Astrophysics (MPA), New Mexico State University, Ohio State University, University of Pittsburgh, University of Portsmouth, Princeton University, the United States Naval Observatory, and the University of Washington.

Table 1. Partial Correlation Coefficients: Lopsidedness and Star Formation

Par. 1	Par. 2	Dependence Removed	Partial Corr. Coeff.
$\log A_1^i$	D_{4000}	...	–0.58
$\log A_1^i$	$H\delta_A$...	0.52
$\log A_1^i$	PC_1	...	–0.60
$\log A_1^i$	$PC_2 - PC_1$...	0.46
$\log A_1^i$	$\log SFR/M_*$...	0.33
$\log A_1^i$	$g - i$...	–0.57
$\log A_1^i$	D_{4000}	$\log M_*, \log \mu_*, C_i$	–0.30
$\log A_1^i$	$H\delta_A$	$\log M_*, \log \mu_*, C_i$	0.27
$\log A_1^i$	PC_1	$\log M_*, \log \mu_*, C_i$	–0.33
$\log A_1^i$	$PC_2 - PC_1$	$\log M_*, \log \mu_*, C_i$	0.22
$\log A_1^i$	$\log SFR/M_*$	$\log M_*, \log \mu_*, C_i$	0.15
$\log A_1^i$	$g - i$	$\log M_*, \log \mu_*, C_i$	–0.21
$\log A_1^i$	$\log M_*$	D_{4000}	–0.14
$\log A_1^i$	$\log \mu_*$	D_{4000}	–0.26
$\log A_1^i$	C_i	D_{4000}	–0.17
$\log A_1^i$	$H\delta_A$	D_{4000}	0.11
$\log A_1^i$	PC_2	...	–0.20

Table 2. Partial Correlation Coefficients: Lopsidedness and Metallicity

Par. 1	Par. 2	Dependence Removed	Partial Corr. Coeff.
$\log A_1^i$	$12 + \log(O/H)$	$\log M_*$	–0.15
$\log A_1^i$	$12 + \log(O/H)$	$\log M_*, \log \mu_*$	–0.10
$\log \mu_*$	$12 + \log(O/H)$	$\log M_*$	0.20
$\log \mu_*$	$12 + \log(O/H)$	$\log A_1^i, \log M_*$	0.19
$\log SFR/M_*$	$12 + \log(O/H)$	$\log M_*$	0.02

Table 3. Partial Correlation Coefficients: Lopsidedness and AGN Activity

Par. 1	Par. 2	Dependence Removed	Partial Corr. Coeff.
$\log A_1^i$	$\log(L[\text{O III}]/M_{BH})$	\dots	0.32
$\log A_1^i$	$\log(L[\text{O III}]/M_{BH})$	$\log M_*$	0.30
$\log A_1^i$	$\log(L[\text{O III}]/M_{BH})$	$\log \mu_*$	0.23
$\log A_1^i$	$\log(L[\text{O III}]/M_{BH})$	C_i	0.19
$\log A_1^i$	$\log(L[\text{O III}]/M_{BH})$	D_{4000}	0.09
$\log A_1^i$	$\log(L[\text{O III}]/M_{BH})$	$\log M_*, \log \mu_*, C_i$	0.22
$\log A_1^i$	$\log(L[\text{O III}]/M_{BH})$	$\log M_*, D_{4000}$	0.09
$\log A_1^i$	$\log(L[\text{O III}]/M_{BH})$	$\log \mu_*, D_{4000}$	0.07
$\log A_1^i$	$\log(L[\text{O III}]/M_{BH})$	C_i, D_{4000}	0.05
$\log A_1^i$	$\log(L[\text{O III}]/M_{BH})$	$\log M_*, \log \mu_*, C_i, D_{4000}$	0.06

REFERENCES

- Adelman-McCarthy, J. K., et al. 2006, *ApJS*, 162, 38
- Angiras, R. A., Jog, C. J., Omar, A., & Dwarakanath, K. S. 2006, *MNRAS*, 369, 1849
- Angiras, R. A., Jog, C. J., Dwarakanath, K. S., & Verheijen, M. A. W. 2007, *MNRAS*, 378, 276
- Baldwin, J. A., Phillips, M. M., & Terlevich, R. 1981, *PASP*, 93, 5
- Bournaud, F., Jog, C. J., & Combes, F. 2005, *A&A*, 437, 69
- Brinchmann, J., Charlot, S., White, S. D. M., Tremonti, C., Kauffmann, G., Heckman, T., & Brinkmann, J. 2004, *MNRAS*, 351, 1151
- Bruzual A., G. 1983, *ApJ*, 273, 105
- Cox, T., Jonsson, P., Somerville, R., Primack, & Dekel, A. 2008, *MNRAS*, 384, 1
- Dalcanton, J. J. 2007, *ApJ*, 658, 941
- Di Matteo, P., Combes, F., Melchior, A., & Semelin, B. 2007, *A&A*, 468, 61
- Di Matteo, T., Colberg, J., Springel, V., Hernquist, L., & Sijacki, D. 2007, *ArXiv e-prints*, 705, arXiv:0705.2269
- Ellison, S. L., Patton, D. R., Simard, L., & McConnachie, A. W. 2008, *AJ*, 135, 1877
- Ellison, S. L., Patton, D. R., Simard, L., & McConnachie, A. W. 2008, *ApJ*, 672, L107
- Fukugita, M., Ichikawa, T., Gunn, J. E., Doi, M., Shimasaku, K., & Schneider, D. P. 1996, *AJ*, 111, 1748
- Gunn, J. E., et al. 1998, *AJ*, 116, 3040
- Gunn, J. E., et al. 2006, *AJ*, 131, 2332 *AJ*, 116, 3040
- Heckman, T. M., Kauffmann, G., Brinchmann, J., Charlot, S., Tremonti, C., & White, S. D. M. 2004, *ApJ*, 613, 109
- Hogg, D. W., Finkbeiner, D. P., Schlegel, D. J., & Gunn, J. E. 2001, *AJ*, 122, 2129
- Hopkins, P. F., Hernquist, L., Cox, T. J., & Keres, D. 2007, *ArXiv e-prints*, 706, arXiv:0706.1243

- Ivezić, Ž., et al. 2004, *Astronomische Nachrichten*, 325, 583
- Jog, C. J. 1999, *ApJ*, 522, 661
- Jog, C. J., & Maybhate, A. 2006, *MNRAS*, 370, 891
- Kauffmann, G., et al. 2003a, *MNRAS*, 341, 33
- Kauffmann, G., et al. 2003b, *MNRAS*, 341, 54
- Kauffmann, G., et al. 2003c, *MNRAS*, 346, 1055
- Kauffmann, G., Heckman, T. M., De Lucia, G., Brinchmann, J., Charlot, S., Tremonti, C., White, S. D. M., & Brinkmann, J. 2006, *MNRAS*, 367, 1394
- Kauffmann, G., et al. 2007, *ApJS*, 173, 357
- Kennicutt, R. C., Jr. 1998, *ApJ*, 498, 541
- Kereš, D., Katz, N., Weinberg, D. H., & Davé, R. 2005, *MNRAS*, 363, 2
- Kewley, L. J., Geller, M. J., & Barton, E. J. 2006, *AJ*, 131, 2004
- Kewley, L. J., Groves, B., Kauffmann, G., & Heckman, T. 2006b, *MNRAS*, 372, 961
- Kornreich, D. A., Lovelace, R. V. E., & Haynes, M. P. 2002, *ApJ*, 580, 705
- Larson, R. B., & Tinsley, B. M. 1978, *ApJ*, 219, 46
- Levine, S. E., & Sparke, L. S. 1998, *ApJ*, 496, L13
- Li, C., Kauffmann, G., Heckman, T., Jing, Y. P., & White, S. D. M. 2007a, *ArXiv e-prints*, 711, arXiv:0711.3792
- Li, C., Kauffmann, G., Heckman, T. M., White, S. D. M., & Jing, Y. P. 2007b, *ArXiv e-prints*, 712, arXiv:0712.0383
- Mapelli, M., Moore, B., & Bland-Hawthorn, J. 2008, *MNRAS*, 388, 697
- Matthews, L. D., van Driel, W., & Gallagher, J. S., III 1998, *AJ*, 116, 1169
- Mihos, J. C., & Hernquist, L. 1996, *ApJ*, 464, 641
- Reichard, T. A., Heckman, T. M., Rudnick, G., Brinchmann, J., & Kauffmann, G. 2008, *ApJ*, 677, 186

- Richter, O.-G., & Sancisi, R. 1994, *A&A*, 290, L9
- Rudnick, G., & Rix, H.-W. 1998, *AJ*, 116, 1163
- Rudnick, G., Rix, H., & Kennicutt, R. C. 2000, *ApJ*, 538, 569
- Smith, J. A., et al. 2002, *AJ*, 123, 2121
- Stoughton, C., et al. 2002, *AJ*, 123, 485
- Swaters, R. A., Schoenmakers, R. H. M., Sancisi, R., & van Albada, T. S. 1999, *MNRAS*, 304, 330
- Toomre, A., & Toomre, J. 1972, *ApJ*, 178, 623
- Tremaine, S., et al. 2002, *ApJ*, 574, 740
- Tremonti, C. A., et al. 2004, *ApJ*, 613, 898
- Tucker, D. L., et al. 2006, *Astronomische Nachrichten*, 327, 821
- Worthey, G., & Ottaviani, D. L. 1997, *ApJS*, 111, 377
- Wild, V., Kauffmann, G., Heckman, T., Charlot, S., Lemson, G., Brinchmann, J., Reichard, T., & Pasquali, A. 2007, *MNRAS*, 381, 543
- Woods, D. F., & Geller, M. J. 2007, *AJ*, 134, 527
- York, D. G., et al. 2000, *AJ*, 120, 1579
- Zaritsky, D., & Rix, H. 1997, *ApJ*, 477, 118